The Plant Cell, Vol. 26: 4547–4560, November 2014, www.plantcell.org

Arabidopsis PIAL1 and 2 Promote SUMO Chain Formation as E4-Type SUMO Ligases and Are Involved in Stress Responses and Sulfur Metabolism[C][W][OPEN]

Konstantin Tomanov,[a] Anja Zeschmann,[b] Rebecca Hermkes,[c] Karolin Eifler,[a,c,1] Ionida Ziba,[a] Michele Grieco,[d] Maria Novatchkova,[e] Kay Hofmann,[f] Holger Hesse,[b] and Andreas Bachmair[a,c,2]

[a] Max F. Perutz Laboratories, Center for Molecular Biology of the University of Vienna, A-1030 Vienna, Austria
[b] Department of Molecular Plant Physiology, Max Planck Institute for Molecular Plant Physiology, D-14476 Potsdam, Germany
[c] Department of Plant Developmental Biology, Max Planck Institute for Plant Breeding Research, D-50829 Cologne, Germany
[d] Department of Ecogenomics and Systems Biology, University of Vienna, A-1090 Vienna, Austria
[e] Research Institute of Molecular Pathology, A-1030 Vienna, Austria
[f] Institute for Genetics, University of Cologne, D-50674 Cologne, Germany

The *Arabidopsis thaliana* genes *PROTEIN INHIBITOR OF ACTIVATED STAT LIKE1* (*PIAL1*) and *PIAL2* encode proteins with SP-RING domains, which occur in many ligases of the small ubiquitin-related modifier (SUMO) conjugation pathway. We show that PIAL1 and PIAL2 function as SUMO ligases capable of SUMO chain formation and require the SUMO-modified SUMO-conjugating enzyme SCE1 for optimal activity. Mutant analysis indicates a role for PIAL1 and 2 in salt stress and osmotic stress responses, whereas under standard conditions, the mutants show close to normal growth. Mutations in PIAL1 and 2 also lead to altered sulfur metabolism. We propose that, together with SUMO chain binding ubiquitin ligases, these enzymes establish a pathway for proteolytic removal of sumoylation substrates.

INTRODUCTION

Sumoylation, the conjugation of the small ubiquitin-related modifier (SUMO) to substrate proteins, is an essential posttranslational modification in plants (reviewed in Novatchkova et al., 2004, 2012; Castro et al., 2012; Mazur and van den Burg, 2012; Flotho and Melchior, 2013; Jentsch and Psakhye, 2013; Xu and Yang, 2013). SUMO activating enzyme (SAE) catalyzes activation of the SUMO carboxyl terminus by formation of a thioester and SUMO transfer to a SUMO conjugating enzyme (SCE). Either alone, or with the help of E3 ligases, SCE links the SUMO carboxyl terminus to lysine ε-amino groups in the substrate. Analysis of mutants suggests that SUMO conjugation is important for responses to a variety of stresses including drought, low temperature, and pathogens (Catala et al., 2007; Conti et al., 2008; Lee et al., 2007; Miura et al., 2007, 2012; Zheng et al., 2012; Li et al., 2013; Zhang et al., 2013) and that sumoylation affects developmental processes such as growth, initiation of flowering, meristem maintenance, gametophyte development, and root architecture (Murtas et al., 2003; Ishida et al., 2009, 2012; van den Burg et al., 2010; Miura et al., 2011; Thangasamy et al., 2011; Ling et al., 2012; Elrouby et al., 2013; Xu et al., 2013; Conti et al., 2014; Son et al., 2014).

The spectrum of identified sumoylation substrates (Budhiraja et al., 2009; Elrouby and Coupland, 2010; López-Torrejón et al., 2013; Miller et al., 2010, 2013) suggests that a wide variety of proteins can be modified by SUMO, with emphasis on proteins of the nucleus. Substrates typically carry a single SUMO moiety. However, the recent discovery of ubiquitin ligases that bind to SUMO chains (Yin et al., 2012b; Elrouby et al., 2013; Sriramachandran and Dohmen, 2014) suggests that SUMO chains have physiological roles as well. However, it is currently unclear how widespread SUMO chains really are, how their formation is regulated, and how they influence biological processes in plants.

In contrast to the analogous ubiquitylation process, which employs a plethora of E3 ligase components to target specific substrates, sumoylation relies on a surprisingly small number of components, contrasting with its broad spectrum of substrates. In particular, SCE, the product of an essential single copy gene in *Arabidopsis thaliana* (Saracco et al., 2007), can directly transfer SUMO to a significant fraction of pathway substrates. To date, only two E3 ligases of the SUMO pathway have been described in *Arabidopsis*, SAP AND MIZ1 (SIZ1) (Miura et al., 2005) and HIGH PLOIDY2 (HPY2) (Ishida et al., 2009; called MMS21 in Huang et al., 2009). Both proteins contain an SP(SIZ-PIAS)-RING (also called a zf-MIZ) domain, which groups them together with mammalian PIAS (protein inhibitor of activated STAT) type SUMO ligases. Whereas HPY2 regulates endoreduplication cycles and affects root development, SIZ1 is best known for involvement in a variety of stress responses (see above).

[1] Current address: Department of Molecular Cell Biology, Leiden University Medical Center, NL-2333 ZA Leiden, The Netherlands.
[2] Address correspondence to andreas.bachmair@univie.ac.at.
The author responsible for distribution of materials integral to the findings presented in this article in accordance with the policy described in the Instructions for Authors (www.plantcell.org) is: Andreas Bachmair (andreas.bachmair@univie.ac.at).
[C] Some figures in this article are displayed in color online but in black and white in the print edition.
[W] Online version contains Web-only data.
[OPEN] Articles can be viewed online without a subscription.
www.plantcell.org/cgi/doi/10.1105/tpc.114.131300

The *Arabidopsis* genome encodes at least two additional proteins with SP-RING domains; we called these proteins PROTEIN INHIBITOR OF ACTIVATED STAT (PIAS) LIKE1 (PIAL1) and 2 and examined their contribution to sumoylation in plants. We find that both function in vitro to enhance the formation of SUMO chains, i.e., SUMO-SUMO isopeptide linkages. Mutant analysis suggests that PIAL1 and 2 contribute to the regulation of salt stress and osmostress responses and are involved in sulfate assimilation and sulfur metabolism. Their functions overlap, but show no obvious redundancy with the previously characterized SUMO ligase SIZ1, which is consistent with the model that SIZ1 preferentially enhances substrate sumoylation, whereas PIALs extend SUMO residues on substrates into chains.

RESULTS

Two *Arabidopsis* Genes Encoding Putative SUMO Ligases

The *Arabidopsis* genome encodes four proteins with an SP-RING (zf-MIZ) domain. Structural studies indicate that this domain mediates binding to the SCE (Yunus and Lima, 2009) to promote SUMO conjugation. Two of the *Arabidopsis* SP-RING-containing proteins were characterized in previous work; to complement this, we studied the physiology and biochemistry of the other two proteins. At1g08910 was called *PIAL1*, and At5g41580 was called *PIAL2*. Their mRNAs were identified via cDNA isolation, showing that the two putative genes are not pseudogenes. The *PIAL2* cDNA was obtained from the RIKEN repository (Seki et al., 2002) and the *PIAL1* cDNA was isolated by reverse transcription of RNA prepared from plants. Sequences of their open reading frames, as obtained from the cDNAs, and protein sequences are shown in Supplemental Figures 1 and 2. The two proteins have similarity to each other (Figure 1; Supplemental Figure 3A). One striking difference between them is the presence of an insertion consisting of seven repeats of 23 amino acids in PIAL1, but not in PIAL2 (Supplemental Figure 3C). PIAL1 and 2 have potential orthologs in other plants, although some plants have only a single gene, as opposed to the two representatives in *Arabidopsis* (Novatchkova et al., 2012). Using the SP-RING sequence for alignment, Figure 1C shows a phylogenetic tree, indicating that plants encode three classes of SP-RING containing SUMO ligases. Branch lengths reflect the number of substitutions (scale bar indicates 0.2% changes per base). Entries from *Arabidopsis* (At), tomato (*Solanum lycopersicum*; Solyc), rice (*Oryza sativa*; Os), and sorghum (*Sorghum bicolor*; Sb) were used for tree building. Bootstrap values are listed in Supplemental Figure 4, and gene candidates from additional species can be found in Novatchkova et al. (2012). The PIAL1 and 2 cDNA sequences differ slightly from previously annotated sequences or gene models (see Supplemental Figure 5 for comparative alignment of proposed PIAL1 intron-exon structures). However, we show in the following that PIAL1 and PIAL2 proteins are functional SUMO ligases in vitro, indicating that the sequences characterized in this work represent authentic gene products. Both genes are expressed at low to moderate levels in a broad range of tissues including young rosette leaves, cauline leaves, and flowers (Supplemental Figure 6). The Univ. of Toronto eFP Browser (Winter et al., 2007) indicates that transcription of *PIAL1* is increased by heat, whereas transcription of *PIAL2* is transiently increased by salt and osmotic stress.

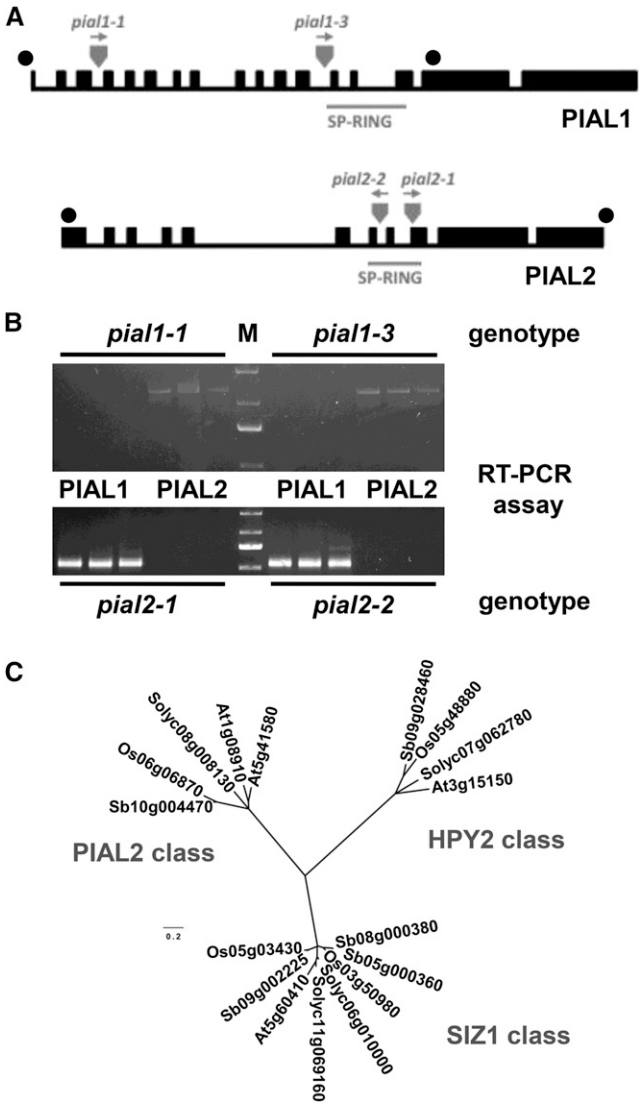

Figure 1. Gene Models, T-DNA Insertion Mutants, and Phylogenetic Relationships of *Arabidopsis* SUMO Ligases.

(A) *PIAL1* and *PIAL2* exon-intron structure based on cDNA versus genomic sequence comparison and position of T-DNA insertions in mutant alleles used in this work. Gray: position of T-DNA insertions and allele designation. Gray underlined: position of SP-RING domain. Black dots indicate position of primers used in **(B)**.

(B) RT-PCR experiment (three technical replicates) to demonstrate absence of full-length mRNA in mutants *pial1-1*, *pial1-3*, *pial2-1*, and *pial2-2*. M, DNA size marker (bands of 3, 2, 1.5, and 1 kb).

(C) Phylogenetic tree based on SP-RING domain sequences indicates presence of three distinct branches of SUMO ligases in plants. At, *Arabidopsis thaliana*; Os, *Oryza sativa*; Sb, *Sorghum bicolor*; Solyc, *Solanum lycopersicum*. For further explanations, see text. Bootstrap values are provided in Supplemental Figure 4.

T-DNA insertions in both genes were obtained from public collections (Sessions et al., 2002; Alonso et al., 2003; Kleinboelting et al., 2012), and we used two independent alleles for assays of this

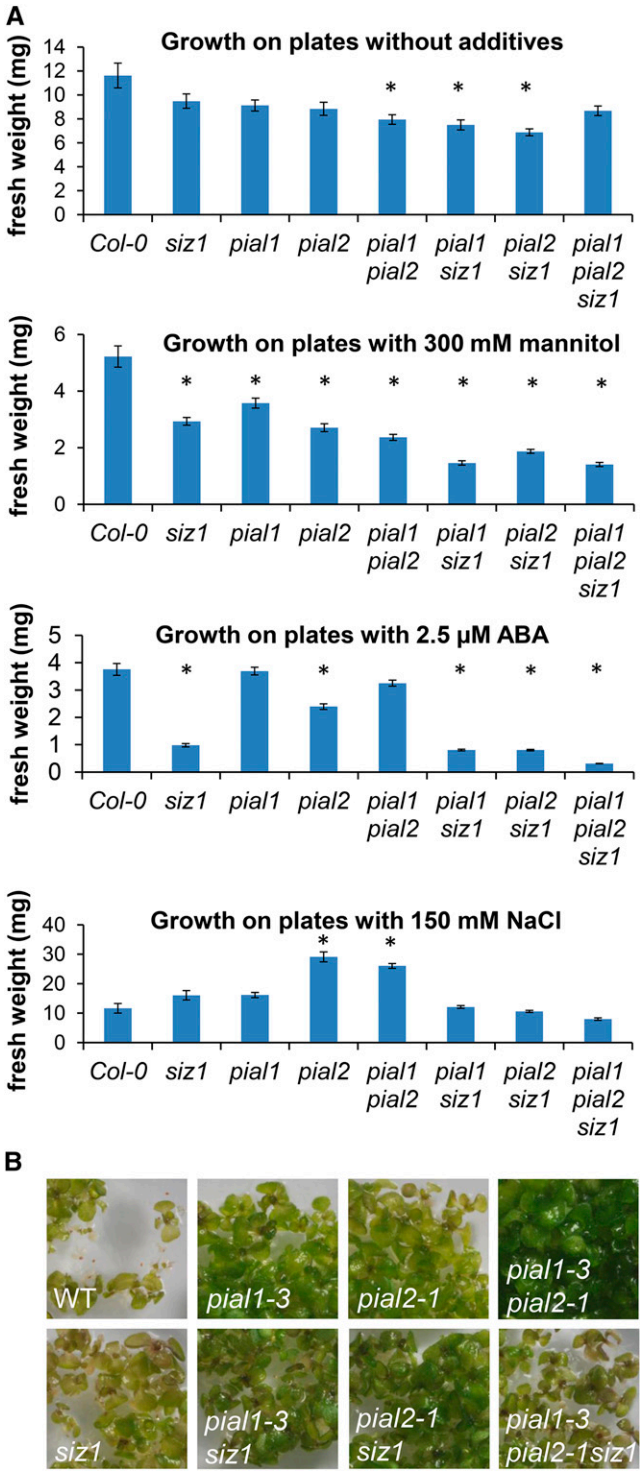

Figure 2. Seedling Growth under Stress Conditions.

(A) Seedlings of the indicated genotypes were germinated and grown on MS plates containing either no additive, 300 mM mannitol, 2.5 µM abscisic acid, or 150 mM NaCl. Seedling fresh weight was determined for size comparison. Results for different mutant alleles did not differ and were pooled for the diagrams. Error bars show SE of the mean, and asterisks indicate significant difference from Columbia-0 reference grown at the same condition ($P < 0.0001$, two-sided *t* test).

(B) Images of plants grown at 150 mM NaCl.

[See online article for color version of this figure.]

work in order to exclude the influence of unintended mutations that might be present in the studied plant lines. Positions of T-DNA inserts are shown as thick arrows in Figure 1A. None of these mutant lines expresses full-length mRNA (Figure 1B; three technical replicates shown). Neither *pial1* or *pial2* single mutants nor double mutants showed any obvious growth difference under standard greenhouse conditions (Supplemental Figure 7). The slightly reduced growth of *pial1 pial2* double mutants on plates at early stages (Figure 2A) does not translate into differences of mature plants on soil. This contrasts with significant growth defects of the previously identified *siz1* mutant. In the *siz1* background, additional mutations in *pial1* and *pial2* lead to a further, albeit small, reduction in size. All mutant combinations with *siz1* are viable (Supplemental Figure 7) and set seed if supplemented with ammonium ions (Park et al., 2011).

Phenotypic Characteristics of *pial* Mutants

Based on the known role of SUMO conjugation in stress responses, and on the finding that *PIAL* expression is stress-responsive, growth under a number of stressful conditions was tested for wild-type and mutant seedlings. Seeds were plated on phytagel medium, and the wet weight of germinated seedlings was determined. A total of 5468 plants were classified, more than 1200 for each condition (Supplemental Table 1). Figure 2A lists growth differences as seedling wet weight. Growth differences were particularly obvious under increased osmotic pressure (300 mM mannitol), upon addition of low doses of abscisic acid (ABA; 2.5 µM), and in presence of 150 mM NaCl. The *pial1 pial2* double mutant grows less well under osmotic stress, and this trend is aggravated by the additional presence of a mutation in *SIZ1*. Likewise, *pial1* and *pial2* augment the ABA hypersensitivity phenotype of *siz1* mutants. A surprising result was obtained in the salt stress experiment. Mutant *pial2* and *pial1 pial2* plantlets were significantly heavier than the wild type under these conditions (Figure 2A). Similar differences were also observed regarding dry weight (Supplemental Table 1). Figure 2B and Supplemental Figure 8 show that *pial1 pial2* double mutants are also greener in presence of 150 mM NaCl than wild-type plants. Chlorophyll fluorescence measurements were performed to relate this latter phenotype to photosystem II (PSII) performance (reviewed in Baker, 2008; Murchie and Lawson, 2013). From the fluorescence yield, two parameters were derived, the maximal quantum yield Fv/Fm commonly used to monitor the stress level in plants, and PSII operating efficiency Fq′/Fm′, which is an estimation of the fraction of absorbed light energy used for photosynthesis. Figure 3 shows that *pial1*, *pial2*, and *pial1 pial2* mutants are significantly better able to maintain PSII activity under salt stress. Both Fv/Fm and Fq′/Fm′ of single mutants even approach the level of unstressed wild-type plants (~0.83 and ~0.6, respectively, under the light conditions of the experiment; Yin et al., 2012a), in accordance with their higher biomass and darker green color. Taken

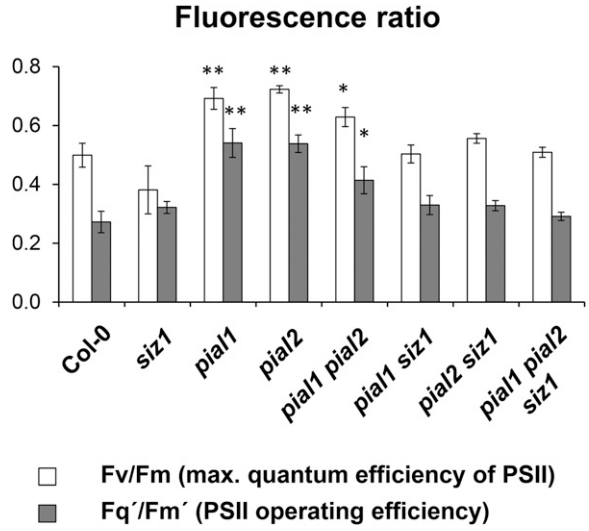

Figure 3. Chlorophyll Fluorescence Measurements to Assess Performance of Photosystem II under Salt Stress.

Plants were grown on plates containing 150 mM NaCl as in Figure 2. Fluorescence images of 2-week-old seedlings were recorded, and ratios Fv/Fm, as well as Fq′/Fm′, were calculated as described in Methods. Results indicate increased PSII performance in *pial1* and *pial2* as well as in *pial1 pial2* double mutants. Asterisks indicate significant differences to the wild type (**P < 0.0001; *P < 0.05; two-sided *t* test).

together, these results show that PIAL1 and PIAL2 affect stress responses. Interaction with SIZ1 may occur in response to ABA but is less likely for the osmotic or salt stress responses.

SUMO Conjugation in *pial* Mutants

We next were interested in global SUMO conjugate levels in mutant plants. Extracts from 2-week-old seedlings were subjected to gel blotting and probed with anti-SUMO1 antibody. Experiments shown in Supplemental Figure 9 indicated that, whereas the wild type and mutants differed in steady state levels of SUMO conjugates, conditions used to probe long-term effects on growth, in particular 300 mM mannitol treatment, gave results that were similar to unstressed samples. This contrasts with previous findings that SUMO conjugate levels change rapidly upon heat treatment (Kurepa et al., 2003). In order to also probe dynamic changes in SUMO conjugate levels, seedlings grown under normal conditions were compared with seedlings after a 1 h 37°C heat shock. Figure 4 shows a diagram of the results (four biological replicates). *pial1 pial2* double mutants have similar or even higher SUMO conjugate levels than the wild type both under normal and under heat stress conditions. As previously published (Miura et al., 2005), *siz1* mutants contain significantly less SUMO conjugates (one-sided *t* test, P < 0.05 and P < 0.005 for normal and heat stress conditions, respectively), and conjugate levels in *siz1* mutants do not rise upon heat stress. In contrast, SUMO conjugate levels in the triple mutant *pial1 pial2 siz1* under heat stress are close to wild-type levels (difference between *siz1* and triple mutant at significance level P = 0.08). To interpret this surprising result, we hypothesize that SUMO conjugation by PIAL1 and PIAL2 is actually part of a desumoylation route, in which PIAL activity to build SUMO chains on monosumoylated substrates leads to their removal, e.g., via SUMO chain-specific ubiquitin ligases (see Discussion). Lack of PIAL1 and 2 may therefore result in increased SUMO conjugate levels under some conditions.

Assessment of Metabolite Differences

Changes in metabolites were also associated with mutations in SUMO ligases. We compared *siz1* mutants to *pial1 pial2* mutants (two different alleles) and to wild-type plants grown on soil under standard greenhouse conditions. Exact values for all metabolites are listed in Supplemental Table 2. Figure 5 shows that *siz1* and *pial1 pial2* mutants differ from the wild type and from each other in the content of many metabolites. For instance, whereas glucose levels in *pial1 pial2* mutants are comparable to the wild type, glucose content is decreased in *siz1*. Conversely, fructose is elevated in *pial1 pial2*, but close to the wild type in *siz1*. Malate content in *pial1 pial2* is in the wild-type range but elevated in *siz1*. Statistical analysis clearly puts *pial1-1 pial2-2* and *pial1-3 pial2-1* double mutants close to each other, and distinct from *siz1*, confirming equivalence of T-DNA insertion alleles and the hypothesis that PIALs and SIZ1 perform distinct functions. Measurement of nitrate content further supports this notion (Figure 6A). Nitrate reductase (NR) is a known substrate of SIZ1-dependent SUMO conjugation and is activated by sumoylation (Park et al., 2011). Increased levels of nitrate in *siz1* mutants are consistent with

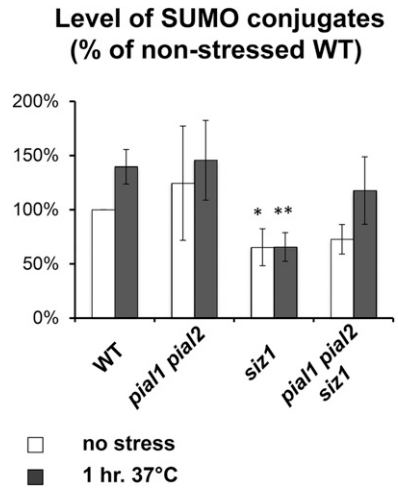

Figure 4. Global SUMO Conjugate Levels in Mutants.

Protein extracts from 2-week-old seedlings were subjected to protein blot and hybridization to anti-SUMO1 antibodies and to protein determination for normalization (Supplemental Figure 9). Results were quantitated to obtain bar diagrams, using Columbia-0 without stress treatment as standard. Plants were subjected to 1 h 37°C heat shock or left at 23°C prior to protein harvest. Error bars indicate SE of the mean of four biological replicates. Significance level: *P < 0.05 and **P < 0.005 (one-sided *t* test, comparison of *siz1* mutant to the wild type of similar treatment).

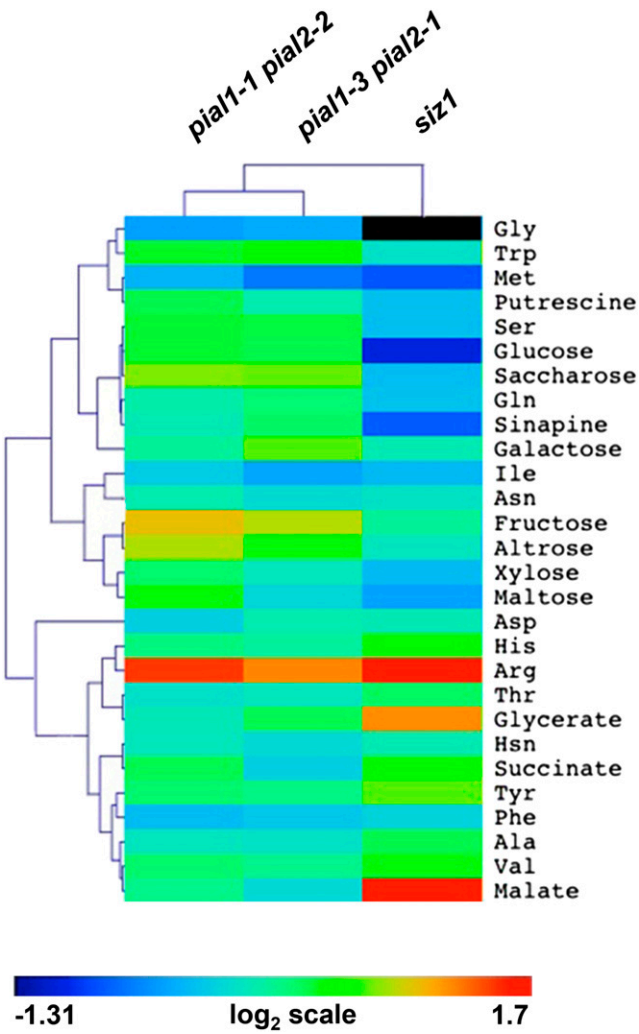

Figure 5. Metabolite Concentrations in SUMO Conjugation Mutants.

The concentration of key metabolites was determined to assess differences in SUMO conjugation mutants. Color coding was performed according to the indicated $\log_2$-scale heat map.

reduced NR activity, as reduced activity may lead to substrate accumulation. In contrast, *pial1 pial2* mutants have nitrate levels slightly below the wild type, suggesting that the influence of PIALs on NR activity may slightly oppose that of SIZ1. The analysis also showed deviations from the wild type in sulfate content, which is particularly pronounced for *pial1 pial2* mutants. We therefore included transcription of key genes of sulfur transport and metabolism in the analysis, using quantitative RT-PCR with primers and gene identifiers listed in Supplemental Table 3. We find that most of the genes of this category are downregulated in *pial1 pial2* mutants (Figure 6B). Figure 5 shows that Met, one of the key sulfur-containing metabolites, is lowered in SUMO conjugation mutants. Figure 7 displays data for another set of sulfur-containing key metabolites, Cys and the Met precursor homocysteine (Homocys), as well as GSH and its precursor γ-glutamyl-cysteine (γ-EC). Whereas Met is decreased, Cys is significantly elevated in *pial1 pial2* mutants. Because Homocys is not elevated, these mutants may have less capacity to convert Cys to Homocys, and subsequently to Met. The tentatively elevated Thr content and the significantly increased contents of Ser, the precursor of Cys, support this interpretation. GSH content is elevated in *pial1 pial2* mutants, as a result of the increased Cys content. GSH precursor γ-EC is also elevated, completing the picture of increased sulfur flow into this redox protective branch. In contrast, *siz1* mutants contain more Homocys, and their decreased Met content may be related to a less efficient conversion of Homocys to Met or higher turnover via *S*-methylmethionine and *S*-adenosylmethionine. GSH levels are closer to normal than in the *pial1 pial2* mutants. In both mutants, however, regulation of sulfur assimilation is apparently perturbed.

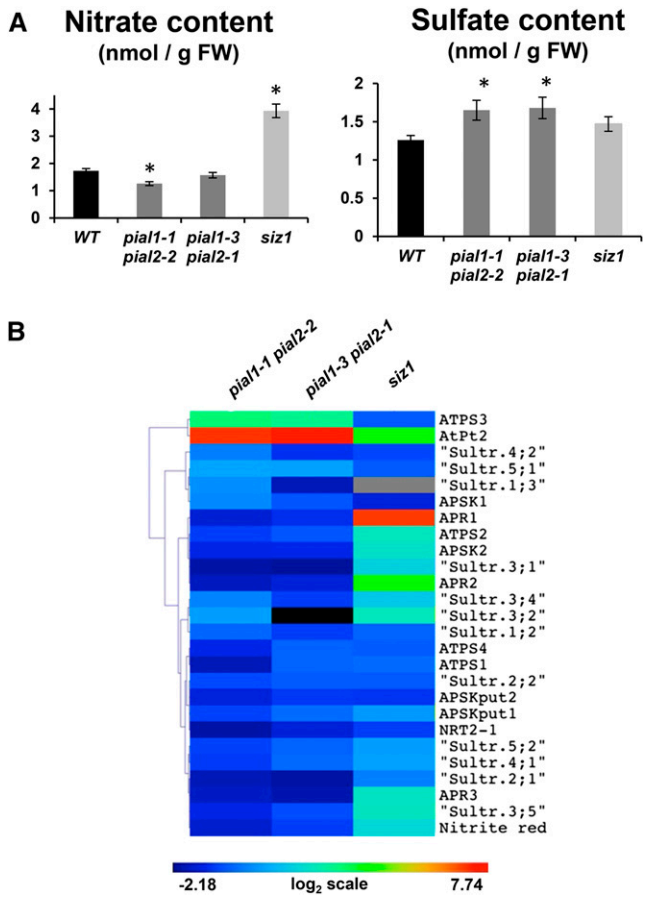

Figure 6. Nitrate and Sulfate Content, and Expression of Key Genes of Sulfur Metabolism.

(A) Concentration of nitrate and sulfate in leaves. Asterisks indicate significant difference from the wild type ($P < 0.05$).

(B) Expression level of key genes related to nitrate and sulfate metabolism, as determined by quantitative RT-PCR, color-coded according to the $\log_2$-scale shown below. ATPS, ATP sulfurylase; AtPt, phosphate transporter; Sultr, sulfate transporter; APSK, APS kinase; APSKput, putative APSK; APR, APS reductase; NRT, nitrate transporter; Nitrite red, nitrite reductase.

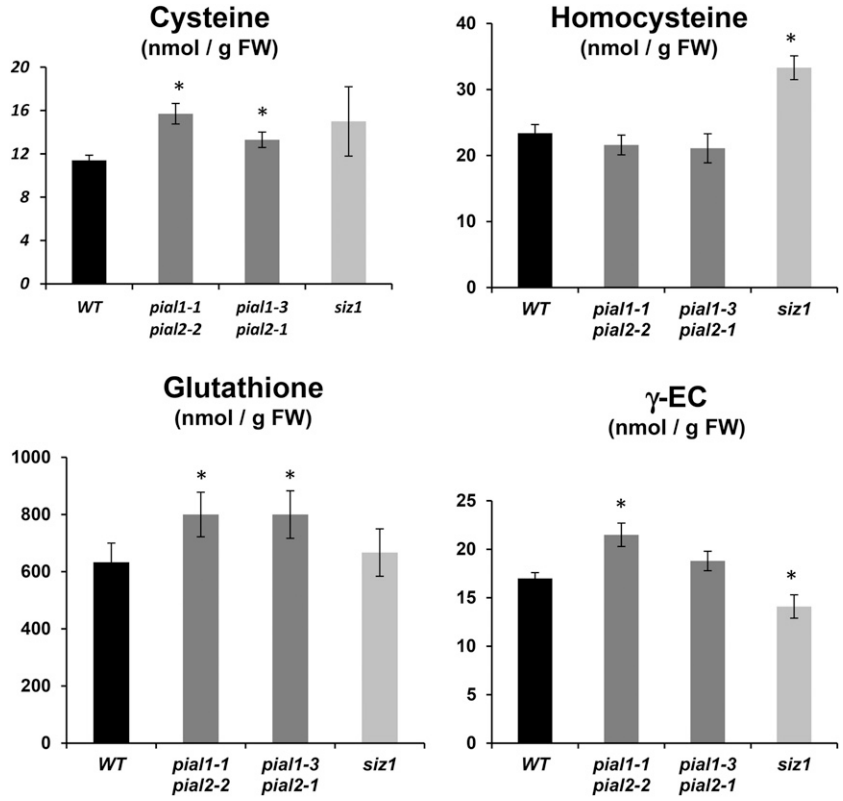

Figure 7. Concentration of Sulfur-Containing Key Metabolites.

The concentration of Cys, Homocys, GSH, and γ-EC was determined in wild-type and mutant leaves. Asterisks indicate significant difference from the wild type ($P < 0.05$).

In Vitro Activity of PIAL Proteins

In order to learn more about the biochemical reactions catalyzed by PIAL1 and PIAL2, full-length and shortened proteins were expressed in *Escherichia coli* cells and used for in vitro SUMO conjugation reactions, together with *E. coli*-produced *Arabidopsis* SAE and SUMO conjugating enzyme (SCE1) (Budhiraja et al., 2009). Figure 8 shows some of the constructs analyzed. We noticed that both PIAL1 and PIAL2 enhanced the normally moderate ability of SCE1 to produce SUMO chains. The activity is displayed by full-length PIAL1 (Figure 8) and PIAL2 (Supplemental Figure 10) and by fragments containing the SP-RING domain together with surrounding protein sequences (amino acids 264 to 445 for PIAL1, called PIAL1M in the following, and 281 to 496 for PIAL2, called PIAL2M). The SP-RING domain alone was catalytically inactive for both proteins. SUMO chain formation is enhanced by PIAL proteins both at low and at high concentration of SCE1 (shown for PIAL2M in Figure 9A; the darkness of the SUMO chain area of the blot was quantified as described in Methods). Furthermore, PIAL2M also enhanced chain formation by SUMO3 (Figure 9B). Mass spectrometry analysis of SUMO1 chains indicated that the same Lys residues were used for SUMO-SUMO bonds as found in reactions with SCE1 alone, namely, Lys-10, Lys-23, and Lys-43. Use of a broad spectrum of SUMO isoforms by PIAL proteins could also be demonstrated by detection of in vitro autosumoylation, which occurred with SUMO1, SUMO3, SUMO5, and SUMO7 (Supplemental Figures 11 and 12). We want to emphasize that autosumoylation of a SUMO ligase in vitro, which generally occurs with any active ligase, may not have in vivo significance. In the context of this work, this reaction supports the notion that PIAL ligases can productively interact with SCE1, which carries a broad variety of SUMO isoforms.

To define functional domains, mutants of the middle sized PIAL2 fragment PIAL2M were tested. Figure 10 and Supplemental Figure 13 show that this protein contains several redundantly acting sequences. The SP-RING motif was mutated by changing two of the Zn^{2+} coordinating Cys residues (shown in bold blue in Supplemental Figure 11A) to Ala. The experiment showed that, surprisingly, destruction of SP-RING functionality does not completely abolish chain-forming activity. Furthermore, a bioinformatic search for potential SUMO interaction motifs (SIMs; Hecker et al., 2006; Vogt and Hofmann, 2012) suggested sequences VFDL and IFDI as candidates (shown as yellow bars in Figure 10A and as red letters in Supplemental Figure 11A). SIMs are short exposed hydrophobic/acidic sequences that can bind to SUMO. The two sequences were mutated either singly, or both to Ala stretches (AAAA; red bars in Figure 10A). Mutation of SIM1 led to a slightly changed spectrum of SUMO chains, and activity of the mutant protein was higher under some experimental conditions (Supplemental Figure 14). However, combined inactivation

of the SP-RING and motif VFDL (SIM1) resulted in complete loss of activity, suggesting that SIM1 and the SP-RING act in part redundantly to catalyze chain formation. A test of deletion variants of PIAL2M (Supplemental Figure 13) showed that deleting the sequence N-terminal to the SP-RING reduced activity and combining this deletion with a SIM1 mutation also led to complete loss of in vitro activity. For mutant protein comparison, two hour in vitro reactions were used as a standard, as shorter time points offer less sensitivity, whereas longer time points may exceed the range of linearity (Supplemental Figure 14).

Analysis of in vitro sumoylation products on Coomassie blue-stained gels indicated two bands that were more prominent in reactions containing PIAL2M than in reactions with SAE and SCE1 only. Mass spectrometry analysis indicated that these bands represent SCE1 linked to SUMO via Lys-15 of SCE1. Immunoblotting with anti SCE1 antibody confirmed this analysis (Figure 11A; the lower SCE1-SUMO band resulted from proteolytic loss of the N-terminal extension that was appended to SUMO for in vitro detection purposes). In order to find out whether SUMO conjugation to Lys-15 of SCE1 is functionally important

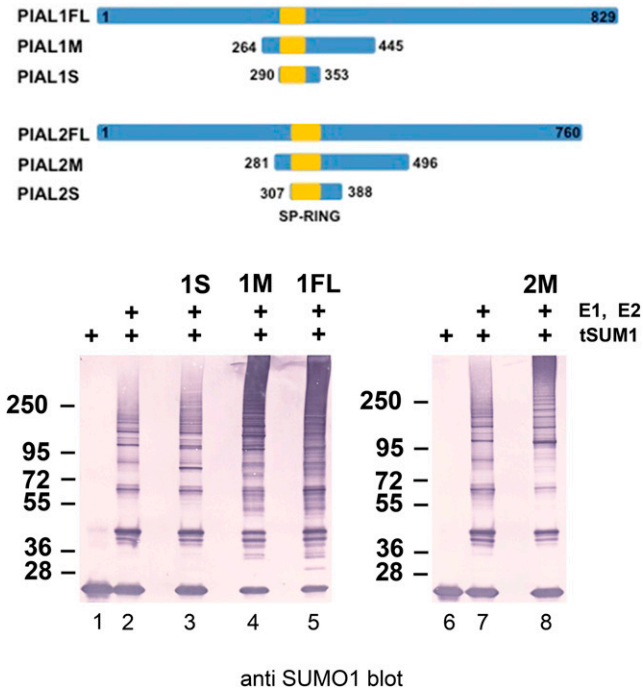

Figure 8. In Vitro Sumoylation Assays with PIAL1 and PIAL2.

Maltose binding protein fusions to PIAL1 and PIAL2 open reading frames and deletion variants (numbers in top panels indicate amino acids contained in the constructs) were used for in vitro SUMO conjugation assays. Reactions were subjected to protein gel blots, and SUMO protein was visualized using antibody against its strep tag. SUMO activating enzyme (E1), SUMO conjugating enzyme (E2), and SUMO1 (with N-terminal tag, tSUM) can generate SUMO chains (lane 2). Chain formation is enhanced by full-length construct PIAL1FL (lane 5) and by the middle-sized fragments PIAL1M and PIAL2M (lanes 4 and 8), but not by a fragment consisting of the SP-RING (in the online version, shown as yellow in the top panel) with little flanking sequence (lane 3).
[See online article for color version of this figure.]

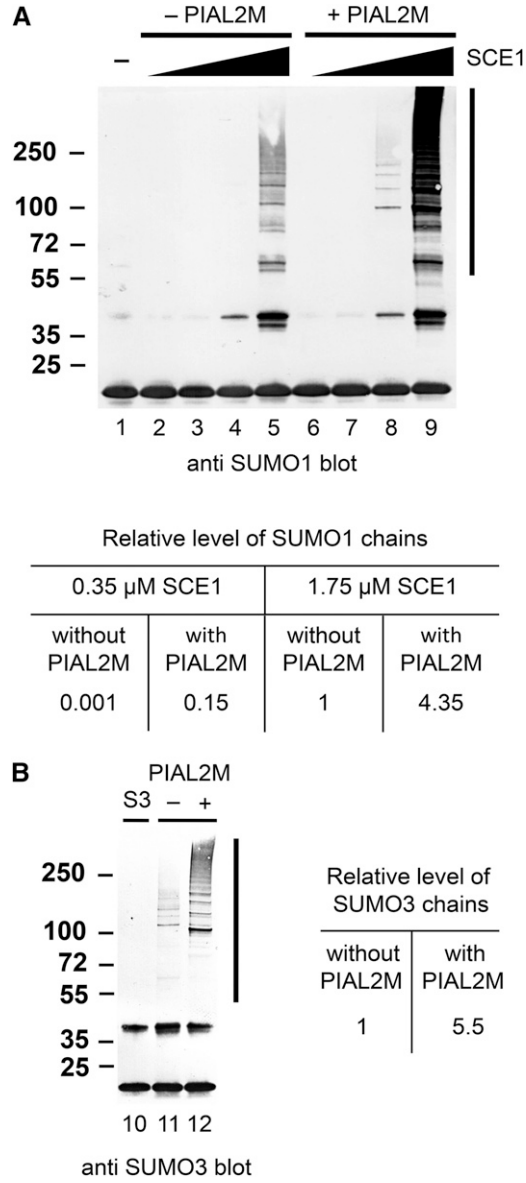

Relative level of SUMO1 chains

0.35 μM SCE1		1.75 μM SCE1	
without PIAL2M	with PIAL2M	without PIAL2M	with PIAL2M
0.001	0.15	1	4.35

Relative level of SUMO3 chains

without PIAL2M	with PIAL2M
1	5.5

Figure 9. Quantitation of SUMO Chain Formation.

(A) Top, in vitro sumoylation reactions were supplied with rising concentrations of SCE1 (lanes 2 and 6, 0.014 μM final concentration; lanes 3 and 7, 0.07 μM; lanes 4 and 8, 0.35 μM; lanes 5 and 9, 1.75 μM). Reactions of lanes 6 to 9 contained 1.5 μM PIAL2M. Reaction products were gel-separated and transferred to a membrane, and SUMO was detected immunologically. Bottom, result of SUMO chain abundance measurements from the blot above (line to the right of the blot indicates size range used for quantification).
(B) PIAL2M also enhances SUMO3 (S3) chain formation. Left, protein gel blot to detect SUMO3 chains after an in vitro reaction. Lane 10, SUMO3 (S3) input without reaction components; lane 11, reaction without PIAL2M; lane 12, reaction in presence of 1.5 μM PIAL2M. Right, quantitation of SUMO chain abundance in analogy to **(A)**.

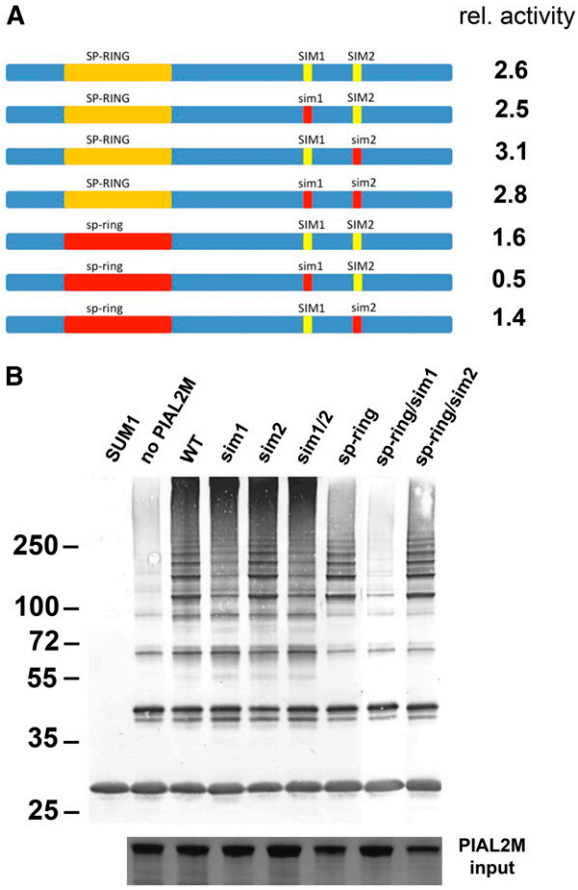

Figure 10. Redundancy of Functional Domains in PIAL2M.

(A) Scheme of constructs and relative activity. In addition to the SP-RING, two potential SIMs were mutated in PIAL2M. Yellow bars indicate intact functional elements and red bars mutated elements. The abundance of SUMO chains in the blot of **(B)** is shown to the right of each construct (values relative to the reaction without PIAL2M protein).

(B) Activity assay (anti SUMO protein gel blot) used to determine relative activity values of **(A)**. Bottom insert shows section of a Coomassie blue-stained gel to document the amount of PIAL2M variant protein added to the reaction.

for SUMO chain formation, an SCE1 K15R mutant was prepared. It could not form significant amounts of SUMO chains in the presence or absence of PIAL2M (Figure 11B). In contrast, its activity to sumoylate the model substrate Nucleosome Assembly Factor (Budhiraja et al., 2009) in vitro was unchanged (Figure 11C). We therefore conclude that SUMO conjugation to SCE1 at position Lys-15 is essential for SUMO chain formation in *Arabidopsis*. Interestingly, a highly active mutant version of PIAL2M (SIM1 Ala substitution mutant of Figure 10 and Supplemental Figure 14) was still able to generate low amounts of SUMO chains with SCE1 K15R. This result may indicate that PIAL ligases have a direct role in SUMO chain formation (preferentially together with SUMO-modified SCE1, but also, less efficiently, with nonmodified SCE1) and that the role of PIALs in chain formation is not restricted to enhanced generation of SUMO-modified SCE1. Nonetheless, SUMO-modified SCE1 is capable of forming SUMO chains without PIALs (its low level presence is apparently responsible for the moderate amounts of SUMO chains formed in absence of PIALs), although it works less efficiently than SUMO-SCE1 and PIAL together.

DISCUSSION

In this work, we characterized two *Arabidopsis* proteins: PIAL1 and PIAL2. They contain an SP-RING domain, which is frequently present in SUMO ligases, and are conserved in the plant kingdom (Novatchkova et al., 2012). Mutants in the respective genes are viable and grow normally under standard greenhouse conditions but show differences under environmental stress conditions. Most remarkably, *pial1 pial2* mutants grow better than the wild type in the presence of 150 mM NaCl (two different T-DNA insertion alleles of both *pial1* and *pial2* were used to exclude effects of potentially present unintended mutations). They are darker green, their PSII performance is close to that of nonstressed wild-type plants, and they have higher fresh weight when grown on plates (Figures 2 and 3). In contrast, these plants are less able to maintain growth under osmotic stress (300 mM mannitol; Figure 2). It remains to be seen how these properties relate to soil-grown plants, which may encounter both stresses at the same time. The SUMO conjugation system has previously been linked to salt stress response, via SUMO-specific proteases OVERLY TOLERANT TO SALT1 (OTS1) and 2 (Conti et al., 2008). Overexpression of either of these two proteases renders *Arabidopsis* plants more resistant to salt stress. OTS and PIAL may therefore act in the same pathway of salt tolerance.

In order to compare PIAL1 and 2 to the known SUMO ligase SIZ1, we generated double and triple mutants. Their analysis established that loss of PIALs in the *siz1* background aggravates the already existing hypersensitivity of *siz1* to the stress hormone ABA (Figure 2A). Double and triple mutant combinations also reduce growth of *siz1* mutants on soil (Supplemental Figure 7), suggesting that *siz1* mutants are particularly sensitive to loss of PIAL function. The analysis of SUMO conjugate levels in the mutants (Figure 4) indicated that mutants in PIAL 1 and 2, in contrast to mutants in SUMO ligase SIZ1, have normal or slightly elevated SUMO conjugate levels. However, combining *siz1* with *pial1* and *pial2* mutations largely reverses the reduced SUMO conjugate levels of *siz1* under heat shock. This is an unusual result for removal of SUMO ligases, for which one might expect a further reduction in SUMO conjugate levels. Although part of this effect might result from compensatory changes in activity of the remaining sumoylation components, we favor an explanation for this finding, as discussed below.

As a further characterization of mutants, we performed a detailed metabolite analysis. Figure 5 indicates a profound difference between *pial1 pial2* and *siz1* mutants. For instance, *siz1* had reduced glucose content, whereas *pial1 pial2* had normal glucose levels. Malate was increased in *siz1* and normal in *pial1 pial2*, whereas fructose was normal in *siz1*, but increased in *pial1 pial2*. A detailed list of all metabolites is presented in Supplemental Table 2.

Figure 6A examines two major nutrient ions: nitrate and sulfate. *siz1* mutants had increased nitrate content, whereas the content was slightly lowered in *pial1 pial2* plants. The increase in *siz1* can be related to the finding (Park et al., 2011) that sumoylation of

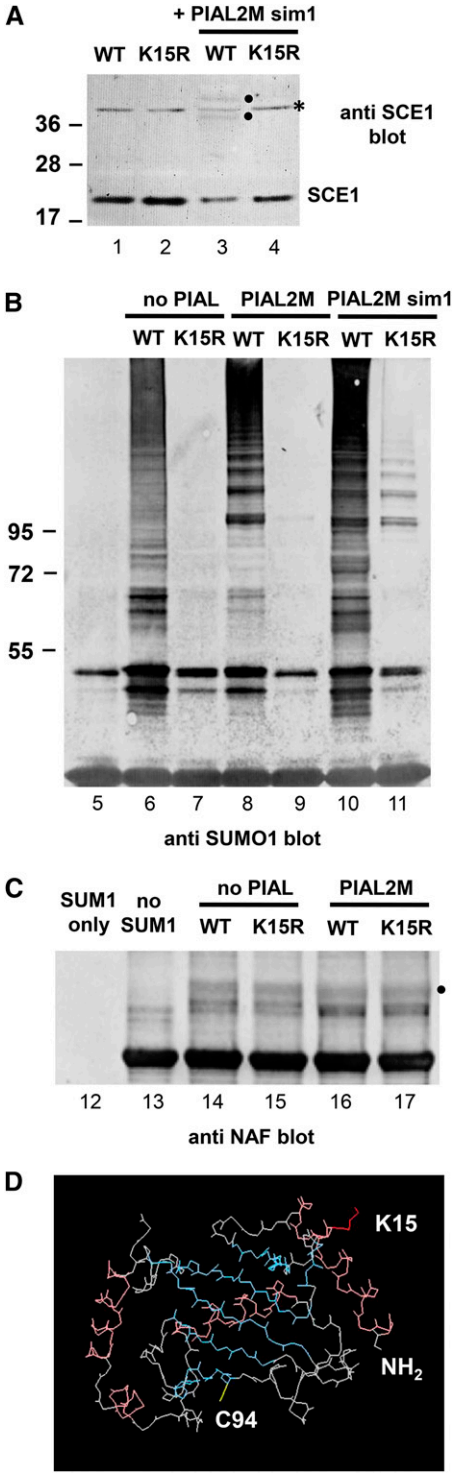

Figure 11. Sumoylation of SCE1 at Lys-15 Is Necessary for SUMO Chain Formation.

(A) The presence of PIAL2M increases abundance of SCE1 sumoylated at Lys-15 (lane 3 versus lane 1). In contrast, SUMO conjugation to SCE1 does not occur if Lys-15 is mutated to Arg (lanes 2 and 4). Dots, SUM1-SCE1 (higher band with intact extension on SUMO1; lower band with proteolytically shortened extension); asterisk, cross-reacting band.

nitrate reductase by SIZ1 activates this enzyme. It is thus plausible that the lack of efficient nitrate reduction is responsible for the accumulation of nitrate. This interpretation is supported by the finding that *siz1* and *siz1 pial* double and triple mutant combinations grow better in presence of additional ammonium ions (Park et al., 2011; data not shown). We conclude from the data that PIAL1 and PIAL2 have only minor influence on nitrate metabolism. The second diagram of Figure 6A shows sulfate levels. The levels were significantly elevated in *pial1 pial2* double mutants, but much less so in *siz1* mutants.

An influence of SUMO conjugation on sulfate metabolism was not previously reported. We therefore gathered more data on components of sulfur-related pathways. Although SUMO conjugation is a posttranslational modification, its perturbation may well affect gene expression. Figure 6B shows gene expression data on sulfate transporters and on key enzymes of sulfur metabolism. Even a first glance leads to the conclusion that there is significant deviation from wild-type expression. Consistent with the more significant deviation of sulfate levels in *pial* double mutants, less gene expression differences are found in the *siz1* mutant. Most genes of sulfur metabolism are downregulated in *pial1 pial2* mutants. Figure 5 demonstrates decreased levels of Met in both *pial1 pial2* double mutants and in *siz1* single mutants. We determined concentrations of further key sulfur containing compounds and their precursors. In particular, Figure 7 shows that *pial1 pial2* mutants had elevated Cys levels. In contrast, an intermediate of the Cys to Met conversion, Homocys, is not elevated in *pial1 pial2* mutants. Future investigations may therefore capitalize on the step from Cys to Homocys as potentially requiring PIAL assistance. *siz1* mutants, in contrast, have significantly increased Homocys levels, so that steps from Homocys to Met may require SIZ1, or enzymes of the Yang cycle might be regulated by sumoylation (Sauter et al., 2013). GSH, as a major component of redox balance, was also investigated in detail. *pial1 pial2* plants had elevated levels, whereas *siz1* mutants did not significantly deviate from the wild type. Thus, the increased flow of Cys into GSH might be an effect of the deregulated Met formation, usage via the Yang cycle, or the deregulation of the enzyme methionine-γ lyase, degrading Met (Jander and Joshi, 2010).

In vitro SUMO conjugation was chosen as a method to characterize PIAL1 and PIAL2 biochemically. All components of the in vitro system were expressed and purified from *E. coli*, based on *Arabidopsis* cDNA sequences (Budhiraja et al., 2009). Figure 8 and Supplemental Figure 10 show that, most significantly, both

(B) SCE1 K15R has a drastically reduced ability to form SUMO chains (lanes 7, 9, and 11 versus 6, 8, and 10). Lane 5 shows SUMO without SAE and SCE1.
(C) SCE1 K15R can catalyze SUMO conjugation to model substrate nucleosome assembly factor (NAF) as efficiently as SCE1 (lanes 14 and 16 versus 15 and 17), and (mono)sumoylation of this substrate is not enhanced by the presence of PIAL2M. Image shows anti NAF blot, with unmodified NAF as the major band. Dot at the right margin indicates NAF-SUMO band.
(D) Peptide backbone and selected side chains of *Arabidopsis* SCE1, modeled from structural data of human UBC9. C94 is the active site Cys residue (yellow), NH_2 indicates the N-terminal end of the peptide chain, and Lys-15 (red) is the Lys residue used for SUMO addition. α-Helical parts are in pink, and β-sheets are in light blue. The rest of the protein backbone is in gray.

PIAL1 and PIAL2 increase the extent of SUMO chain formation in vitro. This property was also characteristic of smaller protein fragments, consisting of the SP-RING domain plus surrounding sequences. The SP-RING alone, in contrast, had no significant activity. The construct containing SP-RING plus surrounding sequences of PIAL2 was used for further characterization (Figures 9 and 10; Supplemental Figures 13 and 14). SUMO chain enhancement was evident both at low concentrations of SUMO conjugating enzyme SCE1 and at high concentrations.

In vitro mutagenesis showed that an intact SP-RING domain is not absolutely essential for SUMO chain-forming activity. Chain-forming activity is decreased, but not abolished, in a mutant with two changes in functionally critical, Zn^{2+}-coordinating residues (Figure 10). A bioinformatics search for additional functional domains identified two potential SUMO interaction motifs (SIMs; called SIM1 and SIM2 in this work), which consist of exposed hydrophobic and acidic residues that mediate SUMO binding. Most likely due to potential redundancy of SUMO binding sites in PIAL2M, which resulted in a high background, we were not able to directly demonstrate that the identified motifs bind to SUMO. However, simultaneous mutation of both SP-RING and SIM1 completely eliminated activity of PIAL2M. Likewise, deletion of the protein part N-terminal to the SP-RING decreased activity and in combination with the SIM1 mutation led to complete elimination of activity (Supplemental Figure 13). We interpret that PIAL2M contains an array of redundantly acting functional elements, and the SP-RING is just one of them.

Testing of PIAL-mediated enhancement of SUMO conjugation to a number of previously identified substrates (Budhiraja et al., 2009) was unsuccessful, suggesting that PIALs may be specialized in extending single SUMO residues on substrates into chains. However, we noticed that PIAL2M catalyzes increased SUMO conjugation to SCE1 (Figure 11A). Mass spectrometry analysis indicated conjugation onto Lys-15 of SCE1. The SCE1 K15R mutant was used to analyze the role of this conjugate in SUMO chain formation. Figure 11B shows that SCE1-(K15)-SUMO is actually essential for chain formation. This poses the perplexing possibility that the role of PIAL in SUMO chain formation could actually be restricted to formation of SUMO-(K15)-SCE1, which then in turn forms SUMO chains all by itself. However, Figure 11B (lane 11) argues against this hypothesis and for a direct role of PIALs, in that high concentrations of PIAL2M (sim1 mutant) were capable of enhancing SUMO chain formation even with the SCE1 K15R mutant. Consistent with this model is the finding that PIAL2M catalyzes chain formation with SUMO3, which is a poor chain former in absence of PIALs (Figure 9B). In any case, an important step in PIAL activity is to enhance SUMO ligation to SCE1. SUMO-SCE1 could act instead of SCE1 as a SUMO donor (by carrying a second SUMO, for transfer to substrates, on its active site Cys) or act as a cofactor in addition to unmodified SCE1 as the SUMO carrier. That Lys-15 of SCE1 might be dispensable for normal SUMO conjugation activity was demonstrated by the reaction shown in Figure 11C, which indicates that monosumoylation of a model substrate occurs with equal efficiency by both SCE1 and the SCE1 K15R mutant. Figure 11D shows the critical Lys-15 residue in an SCE1 structure model, indicating that SUMO conjugation to this residue does not obstruct the active site cleft.

SUMO conjugation to SCE was previously shown in mammals and in yeast, and it changes catalytic properties and "ligase-like" functions of SCE1 (Knipscheer et al., 2008; Klug et al., 2013). The SUMO-modified yeast enzyme participates in SUMO chain formation (Klug et al., 2013). It appears that in plants, additional dedicated SUMO ligases PIAL1 and PIAL2 control and enhance such a chain-forming activity. Because exclusively chain-forming ligases were called E4 enzymes in the ubiquitin conjugation system, we propose to adopt this terminology for PIAL proteins as well.

Which roles can be imagined in vivo for SUMO chains? We propose that SUMO chain formation can lead to removal of SUMO substrates and substrate assemblages. Although the data presented do not allow conclusions about the quantitative importance of such a pathway, this model can explain why *pial1 pial2* mutants contain more SUMO conjugates under certain conditions (e.g., in heat-shocked *siz1* genetic background). In particular, SUMO chains on substrates generate binding sites for a class of ubiquitin ligases and thus channel them into the ubiquitin-proteasome degradation pathway. These latter enzymes have previously been described in animals and in yeast (Yin et al., 2012b; Sriramachandran and Dohmen, 2014). Similar proteins were predicted (Novatchkova et al., 2012) and experimentally demonstrated (Elrouby et al., 2013) in plants as well. Thus, as part of their in vivo activity of extending mono-SUMO into a chain, PIAL proteins may channel SUMO substrates into the ubiquitin pathway, connecting SUMO conjugation to the major proteolytic pathway of the cell.

METHODS

Plant Material and Growth Conditions

Arabidopsis thaliana wild type and mutants were grown in a greenhouse as described (Hubberten et al., 2012); a 16-h photoperiod at a minimum of 200 μmol m^{-2} s^{-1} and a day/night temperature of 20°C/18°C were used. For metabolome analysis, plant material was harvested 5 weeks after sowing in soil. Plant material was pooled, three plants per line and four pools per line. The experiment was repeated to give if possible three independent biological replicates. For seed propagation, plants were either grown in the greenhouse or in controlled environment chambers in 16-h-illumination/8-h-darkness conditions at 23°C. Mutant alleles used were: *pial1-1*, SALK_083748; *pial1-3*, SAIL_738_B09; *pial2-1*, SALK_043892; *pial2-2*, GK_712B09; and *siz1*, SALK_065397.

Growth on Plates

Arabidopsis seedlings were selected on plates containing Murashige and Skoog (MS) medium: 4.3 g/L MS salts, 0.5 g/L MES, 10 g/L sucrose, and 3.2 g/L GelRite, pH 5.7; MS vitamin mix (Sigma-Aldrich) was added after autoclaving. For continuous stress, the plates were supplemented with 300 mM mannitol, 150 mM NaCl, or 2.5 μM ABA, and the seedlings were grown for 2 weeks in long-day conditions. For heat shock stress, plants were grown on MS plates without stress factors for 2 weeks in long-day conditions. The seedlings were transferred to 1 mL liquid MS medium in a 24-well plate, one plant per well. After 24 h, the 24 well plates were floated in a 37°C water bath. After the stress, seedlings were frozen in liquid nitrogen and ground using a Qiagen Tissue Lyser II for 3$\times$ 1 min at 30 shakes/second. Then, 200 μL Buffer B+ (90 mM HEPES, 30 mM DTT, 2% [w/v] SDS, 20 μg/mL pepstatin, and one tablet protease inhibitor cocktail [Roche] per 7 mL buffer, pH 7.5) were added, and the samples

were heated for 6 min at 95°C. Then they were centrifuged for 5 min at 15,000*g*, and the supernatant was used in immunoblot analysis.

RNA Detection

For RT-PCR results shown Figure 1 and Supplemental Figure 6, mRNA was isolated using the RNeasy Plant Mini Kit (Qiagen) with on-column DNase digestion according to the manufacturer's protocol. First-strand DNA synthesis was performed with 140 ng total RNA using the Life Technologies Super Script II reverse transcriptase kit according to the manufacturer's protocol. One microliter of the first-strand reaction was used as a template in a standard PCR with Promega G2 polymerase for 30 cycles. Every reaction was performed in three technical replicates; *UBC9* (At4g27960) was used as a housekeeping gene for comparison. PCR reactions were run for 33 cycles. Primers are listed in Supplemental Table 3.

Chlorophyll Fluorescence Measurements

Plants were grown on plates containing 150 mM NaCl for 3 weeks under long-day conditions at 120 μmol photons m^{-2} s^{-1}. Chlorophyll fluorescence was detected by an Imaging-PAM fluorometer (Walz). Before measurement, plants were incubated in darkness for 10 min. After turning on the measuring light, a saturating pulse (SP; 8000 μmol photons m^{-2} s^{-1}) was applied to determine the Fv/Fm value. Subsequently, an actinic light (134 μmol photons m^{-2} s^{-1}) was turned on and a sequence of SPs was applied (one SP every 30 s) to monitor Fq′/Fm′ (PSII operating efficiency) under steady state illumination.

Vector Construction

A list of vectors is provided as Supplemental Table 4. Standard cloning techniques were used for vector construction. Site-directed mutagenesis was performed with the Agilent QuikChange II kit. For PIAL1 cDNA isolation, seedlings were germinated in liquid half-strength MS medium (six-well microtiter plates). H_2O_2 was added to 10 mM 1 h prior to plant harvest. RNA was extracted (Qiagen RNeasy Plant Mini Kit) and used for reverse transcription (Invitrogen Superscript III) and PCR amplification (TaKaRa LA Taq).

For PIAL2 cloning, RIKEN cDNA clone RAFL16-52-I16 was used as a sequence template (Seki et al., 2002).

Protein Expression and Purification

Recombinant *Arabidopsis* proteins were expressed in *Escherichia coli* using the Rosetta strain (BL21 DE3 pLysS), induced with 1 mM isopropyl β-D-1-thiogalactopyranoside. SUMO isoforms had an N-terminal extension with a poly-His tag (Budhiraja et al., 2009) and were purified using a Ni^{2+}-based affinity chromatography (Qiagen) according to the manufacturer's manual, with the binding buffer supplemented with 10% (v/v) glycerol and 0.5% (v/v) Triton X-100. PIAL1 and PIAL2 variants were N-terminally tagged with maltose binding protein and were purified with an amylose resin (NEB). The two subunits of the E1 (SAE1 and SAE2) were expressed in stoichiometric amounts from a dicistronic construct (Budhiraja et al., 2009). Only SAE2 carried a His-tag. During purification with Ni resin, all buffers were supplemented with 5 mM ATP to promote complex formation. SCE1 was expressed without tag and was extracted by ultracentrifugation of bacterial pellets at 100,000*g* for 1 h after subjecting the pellets to freeze-thaw cycles (Tomanov et al., 2013).

In Vitro SUMO Conjugation Assays

SUMO (14 μM) was incubated with 2 μM SAE, 1.75 μM SCE1 (unless indicated otherwise), and, if appropriate, 1.5 μM ligase for 2 h at 30°C in 20 mM Tris-HCl (pH 7.5), 5 mM $MgCl_2$, and 5 mM ATP.

Immunoblotting and Protein Detection

Proteins were separated using SDS-PAGE and transferred to a polyvinylidene fluoride membrane (Immobilon-P, pore size 0.45 μm; Millipore) by wet blotting for 1 h (1.5 h in case of very large proteins) at 50 V and 4°C. Afterwards, the membrane was blocked for 2 h in 5% skimmed milk powder in Tris-buffered saline (TBS) + 0.05% Tween 20 at room temperature and then washed once with TBS. The primary antibody was diluted in TBS and applied to the membrane overnight at 4°C. The membrane was washed twice with TBS + 0.05% Tween 20 for 5 min and once with TBS only. For conjugated antibodies, the membrane was developed immediately. For nonconjugated antibodies, the secondary antibody was diluted in TBS and applied on the membrane for 2 h at 4°C. Antibodies used were: rabbit anti-*Arabidopsis* SUMO1 (Agrisera; used in 1:2000 dilution), monoclonal mouse anti-maltose binding protein (New England Biolabs; 1:10,000 dilution), AP-conjugated streptavidin (IBA; 1:10,000 dilution), rabbit anti-SCE1 (Budhiraja et al., 2009; 1:100 dilution). After the secondary antibody incubation, the membrane was again washed twice with TBS + 0.05% Tween 20 for 5 min and once with TBS only. For alkaline phosphatase-conjugated secondary antibodies (Sigma-Aldrich anti mouse-IgG or anti rabbit-IgG, both in 1:30,000 dilution): 66 μL 5% Nitro Blue Tetrazolium (Sigma-Aldrich) in 70% *N*,*N*-dimethylformamide and 33 μL 5% 5-bromo-4-chloro-3-indolyl phosphate (Gerbu) in 100% *N*,*N*-dimethylformamide were added to 10 mL TE buffer and applied on the membrane in the dark. For horseradish peroxidase-conjugated antibodies (horseradish peroxidase-conjugated anti rabbit IgG, as provided in the Amersham ECL protein gel blotting kit; GE Healthcare), the membrane was incubated for 2 min in the dark with either Amersham ECL protein gel blotting detection reagents (GE Healthcare) or WesternBright Sirius detection reagents (Pierce). A Fuji medical x-ray film (Fujifilm) was exposed to the membrane and subsequently developed.

Quantitation of Immunoblot Results

For Figure 4 and Supplemental Figure 9, every sample was separated on two gels, one of which was stained with Coomassie Brilliant Blue R 250, and the other was analyzed by immunoblotting. The gels and membranes were scanned and the intensity of their staining was quantified using ImageJ. The anti-SUMO immunoblot intensities were normalized to the Coomassie stain intensity. Samples were compared with the nonstressed Columbia-0 control, which was assigned a value of 1. For the in vitro sumoylation tests (Figures 9 and 10), membranes were scanned and quantified using ImageJ. Sample intensities were compared with the reaction without ligase fragment, which was assigned a value of 1.

Image Processing (SCE1 Structure Data)

The three-dimensional structure of SCE1 was modeled with the ESyPred3D prediction engine (Lambert et al., 2002) using the human homolog UBC9 (PDB ID 2GRN). The three-dimensional structure of the PIAL2 SP-RING (Supplemental Figure 3) was modeled using the bakers' yeast SIZ1 (PDB ID 3E2D).

Metabolite Profiling Using Gas Chromatography Coupled to Mass Spectrometry

For gas chromatography-mass spectrometry analysis, polar metabolite fractions were prepared from 50 mg frozen leaf tissue, which was ground to a fine powder and then extracted with methanol/$CHCl_3$. The metabolite extraction and the preparation of the fraction of polar metabolites by liquid partitioning into water were described earlier (Roessner et al., 2000; Wagner et al., 2003). Metabolite samples were derivatized by methoxyamination, using a 20 mg/mL solution of methoxyamine hydrochloride in pyridine, followed by a subsequent trimethylsilylation step, with

N-methyl-*N*-(trimethylsilyl)-trifluoroacetamide (Fiehn et al., 2000; Roessner et al., 2000). A C12, C15, C19, C22, C28, C32, and C36 *n*-alkane mixture was used for the determination of retention time indices, and chromatographic alignment (Wagner et al., 2003). Ribitol, isoascorbate, and deuterated alanine were added for internal standardization (Kaplan et al., 2004). Samples were injected using splitless mode (1 μL/sample) and analyzed using a quadrupole-type gas chromatography-mass spectrometry system (MD800; ThermoQuest). The chromatograms and mass spectra were evaluated using the MASSLAB software (ThermoQuest), and data were processed using the software TagFinder (Luedemann et al., 2008). Following the procedure of Desbrosses et al. (2005) peak areas, X, were defined to represent the fragment responses (X_i, of fragment i). Fragment responses were normalized to fresh weight and response of the internal standard ribitol using fragment *m/z* = 319, at RI = 1733.7.

Extraction and Metabolite Analysis

Individual soluble thiols were determined as the sum of their reduced and oxidized forms. Fifty milligrams of frozen ground leaf tissue were added to 25.0 mg polyvinylpolypyrrolidone (previously washed with 0.1 M HCl) and 500 μL of 0.1 M HCl. The samples were shaken for 60 min at room temperature. After centrifugation (15 min at 15,777*g*, 4°C), the supernatants were frozen at −20.0°C until reduction/derivatization. The levels of glutathione and cysteine were determined by HPLC-based method after subsequent reduction and derivatization with monobromobimane, as described by Kreft et al. (2003).

Amino acids were determined as described by Kreft et al. (2003). Fifty milligrams of freshly ground frozen plant tissue was extracted for 20 min at 4°C sequentially with 400 μL 80% (v/v), 400 μL 50% (v/v), and 200 μL 80% (v/v) aqueous ethanol (buffered with 2.5 mM HEPES-KOH, pH 6.2). Ethanol/water extracts were subjected to HPLC analysis using a Hyperclone C_{18} BDS column (Phenomenex) connected to an HPLC system (Dionex) (Lindroth and Mopper, 1979).

Quantitative Real-Time PCR

The extraction of total RNA was performed with use of Trizol reagent (Invitrogen). RNA from plant leaves was extracted in 700 μL of the reagent, and after addition of 200 μL chloroform, the polar phase was transferred into a new tube. The aqueous phase was mixed with isopropanol (0.6 volumes) and 3 M sodium acetate (0.2 volumes) to precipitate RNA at room temperature. The RNA precipitate was washed three times with 70% ethanol. The aqueous solution of RNA was treated with DNase (Thermo Scientific) according to the manufacturer's protocol. The cDNA was synthesized from DNA-free RNA by use of oligo-dT_{18} and the RevertAid Premium Reverse Transcriptase (both Thermo Scientific) according to the manufacturer's protocol. PCR was conducted in an optical 384-well plate with an ABI PRISM 7900 HT sequence detection system (Applied Biosystems). Reactions contained 5 μL 2-times SYBR Green Master Mix reagent (Applied Biosystems), 1 μL of 1:5 diluted shoot, 1 μL 1:2.5 diluted root cDNA, and 200 nM of each gene-specific primer. Total reaction volume was 10 μL. The thermal profile used was 50°C for 2 min, 95°C for 10 min, 40 cycles of 95°C for 15 s, and 60°C for 1 min. SDS 2.0 software (Applied Biosystems) was used for data analysis. CT values for genes were normalized to the CT values of ubiquitin. PCR efficiencies were calculated using the LinRegPCR 7.0 program (Ramakers et al., 2003). All primer sequences were designed using the criteria described by Czechowski et al. (2004). RT primer sequences are listed in Supplemental Table 3.

Statistical Analysis

Heat map presentation was performed on the data sets obtained from metabolite profiling with the software package TMEV (Saeed et al., 2003). The data were $\log_2$ transformed before analysis. The *t* tests and error bars in figures were calculated using the algorithm embedded in Microsoft Excel together with add-on Daniel's XL Toolbox.

Accession Numbers

Sequence data from this article (At1g08910 cDNA) can be found in the GenBank/EMBL database under the following accession numbers: Banklt1770634, At1g08910, KP067953; PIAL1, At1g08910; PIAL2, At5g41580; and SIZ1, At5g60410.

Supplemental Data

The following materials are available in the online version of this article.

Supplemental Figure 1. Open Reading Frame and Protein Sequence of PIAL1 as Determined by Sequencing of cDNAs.

Supplemental Figure 2. Open Reading Frame and Protein Sequence of PIAL2 as Determined by Sequencing of cDNAs.

Supplemental Figure 3. Alignment and Structure of SP-RING Proteins.

Supplemental Figure 4. Phylogenetic Tree of SP-RING-Containing Plant Proteins.

Supplemental Figure 5. Published Exon-Intron Structures of PIAL1.

Supplemental Figure 6. Expression of PIAL1 and PIAL2 in Different Tissues.

Supplemental Figure 7. Growth Habit of SUMO Ligase Mutants.

Supplemental Figure 8. Images of Mutant Plants Grown under Various Stresses.

Supplemental Figure 9. Protein Blots and Coomassie-Stained Gels Used to Assess Global SUMO Conjugate Levels.

Supplemental Figure 10. PIAL2, but Not SIZ1, Catalyzes SUMO Chain Formation.

Supplemental Figure 11. In Vitro Autosumoylation of PIAL2.

Supplemental Figure 12. Autosumoylation of PIAL2M Indicates Interaction with SUMO1, SUMO3, SUMO5, and SUMO7.

Supplemental Figure 13. Deletion Analysis of PIAL2.

Supplemental Figure 14. Kinetics of in Vitro SUMO Chain Formation.

Supplemental Table 1. Number of Seedlings Used for Weight Determination and Dry Weight of Seedlings.

Supplemental Table 2. Metabolite Concentrations.

Supplemental Table 3. Primer Sequences Used for qRT-PCR.

Supplemental Table 4. Vectors Used in This Work.

ACKNOWLEDGMENTS

We thank Dorothea Anrather for expert mass spectrometry analysis, Andrea Pichler for advice on in vitro sumoylation reactions, and Ruchika Budhiraja, Josef Fischböck, Teresa Gerber, Philipp Obermayr, and Sebastian Schneider for contributions to the experiments.

AUTHOR CONTRIBUTIONS

A.B., H.H., and K.T. designed the experiments. M.N. and K.H. carried out bioinformatics analyses. K.T., A.Z., R.H., K.E., I.Z., and M.G. performed experiments and contributed to experimental design and interpretation. A.B., H.H., and K.T. wrote the article.

Received August 21, 2014; revised October 20, 2014; accepted November 1, 2014; published November 18, 2014.

REFERENCES

Alonso, J.M., et al. (2003). Genome-wide insertional mutagenesis of *Arabidopsis thaliana*. Science **301:** 653–657.

Baker, N.R. (2008). Chlorophyll fluorescence: a probe of photosynthesis in vivo. Annu. Rev. Plant Biol. **59:** 89–113.

Budhiraja, R., Hermkes, R., Müller, S., Schmidt, J., Colby, T., Panigrahi, K., Coupland, G., and Bachmair, A. (2009). Substrates related to chromatin and to RNA-dependent processes are modified by Arabidopsis SUMO isoforms that differ in a conserved residue with influence on desumoylation. Plant Physiol. **149:** 1529–1540.

Castro, P.H., Tavares, R.M., Bejarano, E.R., and Azevedo, H. (2012). SUMO, a heavyweight player in plant abiotic stress responses. Cell. Mol. Life Sci. **69:** 3269–3283.

Catala, R., Ouyang, J., Abreu, I.A., Hu, Y., Seo, H., Zhang, X., and Chua, N.-H. (2007). The Arabidopsis E3 SUMO ligase SIZ1 regulates plant growth and drought responses. Plant Cell **19:** 2952–2966.

Conti, L., Nelis, S., Zhang, C., Woodcock, A., Swarup, R., Galbiati, M., Tonelli, C., Napier, R., Hedden, P., Bennett, M., and Sadanandom, A. (2014). Small Ubiquitin-like Modifier protein SUMO enables plants to control growth independently of the phytohormone gibberellin. Dev. Cell **28:** 102–110.

Conti, L., Price, G., O'Donnell, E., Schwessinger, B., Dominy, P., and Sadanandom, A. (2008). Small ubiquitin-like modifier proteases OVERLY TOLERANT TO SALT1 and -2 regulate salt stress responses in *Arabidopsis*. Plant Cell **20:** 2894–2908.

Czechowski, T., Bari, R.P., Stitt, M., Scheible, W.R., and Udvardi, M.K. (2004). Real-time RT-PCR profiling of over 1400 Arabidopsis transcription factors: unprecedented sensitivity reveals novel root- and shoot-specific genes. Plant J. **38:** 366–379.

Desbrosses, G.G., Kopka, J., and Udvardi, M.K. (2005). *Lotus japonicus* metabolic profiling. Development of gas chromatography-mass spectrometry resources for the study of plant-microbe interactions. Plant Physiol. **137:** 1302–1318.

Elrouby, N., Bonequi, M.V., Porri, A., and Coupland, G. (2013). Identification of Arabidopsis SUMO-interacting proteins that regulate chromatin activity and developmental transitions. Proc. Natl. Acad. Sci. USA **110:** 19956–19961.

Elrouby, N., and Coupland, G. (2010). Proteome-wide screens for small ubiquitin-like modifier (SUMO) substrates identify Arabidopsis proteins implicated in diverse biological processes. Proc. Natl. Acad. Sci. USA **107:** 17415–17420.

Fiehn, O., Kopka, J., Dörmann, P., Altmann, T., Trethewey, R.N., and Willmitzer, L. (2000). Metabolite profiling for plant functional genomics. Nat. Biotechnol. **18:** 1157–1161.

Flotho, A., and Melchior, F. (2013). Sumoylation: a regulatory protein modification in health and disease. Annu. Rev. Biochem. **82:** 357–385.

Hecker, C.M., Rabiller, M., Haglund, K., Bayer, P., and Dikic, I. (2006). Specification of SUMO1- and SUMO2-interacting motifs. J. Biol. Chem. **281:** 16117–16127.

Huang, L., Yang, S., Zhang, S., Liu, M., Lai, J., Qi, Y., Shi, S., Wang, J., Wang, Y., Xie, Q., and Yang, C. (2009). The Arabidopsis SUMO E3 ligase AtMMS21, a homologue of NSE2/MMS21, regulates cell proliferation in the root. Plant J. **60:** 666–678.

Hubberten, H.-M., Drozd, A., Tran, B.V., Hesse, H., and Hoefgen, R. (2012). Local and systemic regulation of sulfur homeostasis in roots of *Arabidopsis thaliana.* Plant J. **72:** 625–635.

Ishida, T., Fujiwara, S., Miura, K., Stacey, N., Yoshimura, M., Schneider, K., Adachi, S., Minamisawa, K., Umeda, M., and Sugimoto, K. (2009). SUMO E3 ligase HIGH PLOIDY2 regulates endocycle onset and meristem maintenance in Arabidopsis. Plant Cell **21:** 2284–2297.

Ishida, T., Yoshimura, M., Miura, K., and Sugimoto, K. (2012). MMS21/HPY2 and SIZ1, two Arabidopsis SUMO E3 ligases, have distinct functions in development. PLoS ONE **7:** e46897.

Jander, G., and Joshi, V. (2010). Recent progress in deciphering the biosynthesis of aspartate-derived amino acids in plants. Mol. Plant **3:** 54–65.

Jentsch, S., and Psakhye, I. (2013). Control of nuclear activities by substrate-selective and protein-group SUMOylation. Annu. Rev. Genet. **47:** 167–186.

Kaplan, F., Kopka, J., Haskell, D.W., Zhao, W., Schiller, K.C., Gatzke, N., Sung, D.Y., and Guy, C.L. (2004). Exploring the temperature-stress metabolome of Arabidopsis. Plant Physiol. **136:** 4159–4168.

Kleinboelting, N., Huep, G., Kloetgen, A., Viehoever, P., and Weisshaar, B. (2012). GABI-Kat SimpleSearch: new features of the *Arabidopsis thaliana* T-DNA mutant database. Nucleic Acids Res. **40:** D1211–D1215.

Klug, H., Xaver, M., Chaugule, V.K., Koidl, S., Mittler, G., Klein, F., and Pichler, A. (2013). Ubc9 sumoylation controls SUMO chain formation and meiotic synapsis in *Saccharomyces cerevisiae*. Mol. Cell **50:** 625–636.

Knipscheer, P., Flotho, A., Klug, H., Olsen, J.V., van Dijk, W.J., Fish, A., Johnson, E.S., Mann, M., Sixma, T.K., and Pichler, A. (2008). Ubc9 sumoylation regulates SUMO target discrimination. Mol. Cell **31:** 371–382.

Kreft, O., Hoefgen, R., and Hesse, H. (2003). Functional analysis of cystathionine γ-synthase in genetically engineered potato plants. Plant Physiol. **131:** 1843–1854.

Kurepa, J., Walker, J.M., Smalle, J., Gosink, M.M., Davis, S.J., Durham, T.L., Sung, D.Y., and Vierstra, R.D. (2003). The small ubiquitin-like modifier (SUMO) protein modification system in Arabidopsis. Accumulation of SUMO1 and -2 conjugates is increased by stress. J. Biol. Chem. **278:** 6862–6872.

Lambert, C., Léonard, N., De Bolle, X., and Depiereux, E. (2002). ESyPred3D: Prediction of proteins 3D structures. Bioinformatics **18:** 1250–1256.

Lee, J., et al. (2007). Salicylic acid-mediated innate immunity in Arabidopsis is regulated by SIZ1 SUMO E3 ligase. Plant J. **49:** 79–90.

Li, Z., Hu, Q., Zhou, M., Vandenbrink, J., Li, D., Menchyk, N., Reighard, S., Norris, A., Liu, H., Sun, D., and Luo, H. (2013). Heterologous expression of OsSIZ1, a rice SUMO E3 ligase, enhances broad abiotic stress tolerance in transgenic creeping bentgrass. Plant Biotechnol. J. **11:** 432–445.

Lindroth, P., and Mopper, K. (1979). High performance liquid chromatographic determination of subpicomole amounts of amino acids by precolumn fluorescence derivatization with *o*-phthaldialdehyde. Anal. Chem. **51:** 1667–1674.

Ling, Y., Zhang, C., Chen, T., Hao, H., Liu, P., Bressan, R.A., Hasegawa, P.M., Jin, J.B., and Lin, J. (2012). Mutation in SUMO E3 ligase, SIZ1, disrupts the mature female gametophyte in Arabidopsis. PLoS ONE **7:** e29470.

López-Torrejón, G., Guerra, D., Catalá, R., Salinas, J., and del Pozo, J.C. (2013). Identification of SUMO targets by a novel proteomic approach in plants. J. Integr. Plant Biol. **55:** 96–107.

Luedemann, A., Strassburg, K., Erban, A., and Kopka, J. (2008). TagFinder for the quantitative analysis of gas chromatography—mass spectrometry (GC-MS)-based metabolite profiling experiments. Bioinformatics **24:** 732–737.

Mazur, M.J., and van den Burg, H.A. (2012). Global SUMO proteome responses guide gene regulation, mRNA biogenesis, and plant stress responses. Front. Plant Sci. **3:** 215.

Miller, M.J., Barrett-Wilt, G.A., Hua, Z., and Vierstra, R.D. (2010). Proteomic analyses identify a diverse array of nuclear processes affected by small ubiquitin-like modifier conjugation in Arabidopsis. Proc. Natl. Acad. Sci. USA **107:** 16512–16517.

Miller, M.J., Scalf, M., Rytz, T.C., Hubler, S.L., Smith, L.M., and Vierstra, R.D. (2013). Quantitative proteomics reveals factors regulating RNA biology as dynamic targets of stress-induced SUMOylation in Arabidopsis. Mol. Cell. Proteomics **12:** 449–463.

Miura, K., Jin, J.B., Lee, J., Yoo, C.Y., Stirm, V., Miura, T., Ashworth, E.N., Bressan, R.A., Yun, D.J., and Hasegawa, P.M. (2007). SIZ1-mediated sumoylation of ICE1 controls CBF3/DREB1A expression and freezing tolerance in Arabidopsis. Plant Cell **19:** 1403–1414.

Miura, K., Lee, J., Gong, Q., Ma, S., Jin, J.B., Yoo, C.Y., Miura, T., Sato, A., Bohnert, H.J., and Hasegawa, P.M. (2011). SIZ1 regulation of phosphate starvation-induced root architecture remodeling involves the control of auxin accumulation. Plant Physiol. **155:** 1000–1012.

Miura, K., Okamoto, H., Okuma, E., Shiba, H., Kamada, H., Hasegawa, P.M., and Murata, Y. (2012). SIZ1 deficiency causes reduced stomatal aperture and enhanced drought tolerance via controlling salicylic acid-induced accumulation of reactive oxygen species in Arabidopsis. Plant J. **73:** 91–104.

Miura, K., Rus, A., Sharkhuu, A., Yokoi, S., Karthikeyan, A.S., Raghothama, K.G., Baek, D., Koo, Y.D., Jin, J.B., Bressan, R.A., Yun, D.J., and Hasegawa, P.M. (2005). The Arabidopsis SUMO E3 ligase SIZ1 controls phosphate deficiency responses. Proc. Natl. Acad. Sci. USA **102:** 7760–7765.

Murchie, E.H., and Lawson, T. (2013). Chlorophyll fluorescence analysis: a guide to good practice and understanding some new applications. J. Exp. Bot. **64:** 3983–3998.

Murtas, G., Reeves, P.H., Fu, Y.F., Bancroft, I., Dean, C., and Coupland, G. (2003). A nuclear protease required for flowering-time regulation in Arabidopsis reduces the abundance of SMALL UBIQUITIN-RELATED MODIFIER conjugates. Plant Cell **15:** 2308–2319.

Novatchkova, M., Budhiraja, R., Coupland, G., Eisenhaber, F., and Bachmair, A. (2004). SUMO conjugation in plants. Planta **220:** 1–8.

Novatchkova, M., Tomanov, K., Hofmann, K., Stuible, H.-P., and Bachmair, A. (2012). Update on sumoylation: defining core components of the plant SUMO conjugation system by phylogenetic comparison. New Phytol. **195:** 23–31.

Park, B.S., Song, J.T., and Seo, H.S. (2011). Arabidopsis nitrate reductase activity is stimulated by the E3 SUMO ligase AtSIZ1. Nat. Commun. **2:** 400.

Ramakers, C., Ruijter, J.M., Deprez, R.H.L., and Moorman, A.F.M. (2003). Assumption-free analysis of quantitative real-time polymerase chain reaction (PCR) data. Neurosci. Lett. **339:** 62–66.

Roessner, U., Wagner, C., Kopka, J., Trethewey, R.N., and Willmitzer, L. (2000). Technical advance: simultaneous analysis of metabolites in potato tuber by gas chromatography-mass spectrometry. Plant J. **23:** 131–142.

Saracco, S.A., Miller, M.J., Kurepa, J., and Vierstra, R.D. (2007). Genetic analysis of SUMOylation in Arabidopsis: conjugation of SUMO1 and SUMO2 to nuclear proteins is essential. Plant Physiol. **145:** 119–134.

Saeed, A.I., et al. (2003). TM4: a free, open-source system for microarray data management and analysis. Biotechniques **34:** 374–378.

Sauter, M., Moffatt, B., Saechao, M.C., Hell, R., and Wirtz, M. (2013). Methionine salvage and S-adenosylmethionine: essential links between sulfur, ethylene and polyamine biosynthesis. Biochem. J. **451:** 145–154.

Seki, M., et al. (2002). Functional annotation of a full-length Arabidopsis cDNA collection. Science **296:** 141–145.

Sessions, A., et al. (2002). A high-throughput Arabidopsis reverse genetics system. Plant Cell **14:** 2985–2994.

Son, G.H., Park, B.S., Song, J.T., and Seo, H.S. (2014). FLC-mediated flowering repression is positively regulated by sumoylation. J. Exp. Bot. **65:** 339–351.

Sriramachandran, A.M., and Dohmen, R.J. (2014). SUMO-targeted ubiquitin ligases. Biochim. Biophys. Acta **1843:** 75–85.

Thangasamy, S., Guo, C.L., Chuang, M.H., Lai, M.H., Chen, J., and Jauh, G.Y. (2011). Rice SIZ1, a SUMO E3 ligase, controls spikelet fertility through regulation of anther dehiscence. New Phytol. **189:** 869–882.

Tomanov, K., Hardtke, C., Budhiraja, R., Hermkes, R., Coupland, G., and Bachmair, A. (2013). Small ubiquitin-like modifier conjugating enzyme with active site mutation acts as dominant negative inhibitor of SUMO conjugation in Arabidopsis. J. Integr. Plant Biol. **55:** 75–82.

van den Burg, H.A., Kini, R.K., Schuurink, R.C., and Takken, F.L. (2010). Arabidopsis small ubiquitin-like modifier paralogs have distinct functions in development and defense. Plant Cell **22:** 1998–2016.

Vogt, B., and Hofmann, K. (2012). Bioinformatical detection of recognition factors for ubiquitin and SUMO. Methods Mol. Biol. **832:** 249–261.

Wagner, C., Sefkow, M., and Kopka, J. (2003). Construction and application of a mass spectral and retention time index database generated from plant GC/EI-TOF-MS metabolite profiles. Phytochemistry **62:** 887–900.

Winter, D., Vinegar, B., Nahal, H., Ammar, R., Wilson, G.V., and Provart, N.J. (2007). An "Electronic Fluorescent Pictograph" browser for exploring and analyzing large-scale biological data sets. PLoS ONE **2:** e718.

Yin, L., Fristedt, R., Herdean, A., Solymosi, K., Bertrand, M., Andersson, M.X., Mamedov, F., Vener, A.V., Schoefs, B., and Spetea, C. (2012a). Photosystem II function and dynamics in three widely used *Arabidopsis thaliana* accessions. PLoS ONE **7:** e46206.

Yin, Y., Seifert, A., Chua, J.S., Maure, J.F., Golebiowski, F., and Hay, R.T. (2012b). SUMO-targeted ubiquitin E3 ligase RNF4 is required for the response of human cells to DNA damage. Genes Dev. **26:** 1196–1208.

Yunus, A.A., and Lima, C.D. (2009). Structure of the Siz/PIAS SUMO E3 ligase Siz1 and determinants required for SUMO modification of PCNA. Mol. Cell **35:** 669–682.

Xu, P., and Yang, C. (2013). Emerging role of SUMOylation in plant development. Plant Signal. Behav. **8:** e24727.

Xu, P., Yuan, D., Liu, M., Li, C., Liu, Y., Zhang, S., Yao, N., and Yang, C. (2013). AtMMS21, an SMC5/6 complex subunit, is involved in stem cell niche maintenance and DNA damage responses in Arabidopsis roots. Plant Physiol. **161:** 1755–1768.

Zhang, S., Qi, Y., Liu, M., and Yang, C. (2013). SUMO E3 ligase AtMMS21 regulates drought tolerance in *Arabidopsis thaliana*. J. Integr. Plant Biol. **55:** 83–95.

Zheng, Y., Schumaker, K.S., and Guo, Y. (2012). Sumoylation of transcription factor MYB30 by the small ubiquitin-like modifier E3 ligase SIZ1 mediates abscisic acid response in *Arabidopsis thaliana*. Proc. Natl. Acad. Sci. USA **109:** 12822–12827.